Liquid Crystals
Publication details, including instructions for authors and subscription information:
http://www.informaworld.com/smpp/title~content=t713926090

Synthesis, micro structure, and thermal stability of side chain liquid crystalline polysiloxane polymers with an oligo (ethylene oxide) unit in the side chain

Guo-Ping Chang-chien[a]; Jen-Feng Kuo[b]
[a] Department of Chemical Engineering, Cheng-Shiu College of Technology, Taiwan, China [b] Department of Chemical Engineering, National Cheng-Kung University, Tainan, Taiwan, China

To cite this Article Chang-chien, Guo-Ping and Kuo, Jen-Feng(1996) 'Synthesis, micro structure, and thermal stability of side chain liquid crystalline polysiloxane polymers with an oligo (ethylene oxide) unit in the side chain', Liquid Crystals, 20: 6, 705 — 714
To link to this Article: DOI: 10.1080/02678299608033163
URL: http://dx.doi.org/10.1080/02678299608033163

LIQUID CRYSTALS, 1996, VOL. 20, NO. 6, 705-714

Synthesis, micro structure, and thermal stability of side chain liquid crystalline polysiloxane polymers with an oligo (ethylene oxide) unit in the side chain

by GUO-PING CHANG-CHIEN*
Department of Chemical Engineering, Cheng-Shiu College of Technology, Kaohsiung, Taiwan 80741, China

and JEN-FENG KUO
Department of Chemical Engineering, National Cheng-Kung University, Tainan, Taiwan 70101, China

(*Received 19 October 1995; accepted 14 November 1995*)

A series of new alkene monomers [MS3BDBE*n*, $n=1$-3] containing 4-oligo (ethylene oxide) monomethyl ether 4-biphenyl ether carboxyl benzoate as terminal groups were synthesized. These polymers were prepared by grafting these monomers onto the poly(methylhydrosiloxane) (PMHS) backbone. The transition temperatures, liquid crystalline textures, and thermal stability of the polysiloxane polymers have been determined by thermal data, by optical texture, and by X-ray diffraction patterns. Polymers PS3BDBE*n* showed smectic or smectic and nematic phases which were not analogous to their precursor nematic monomers. The terminal length of the polymers affects not only the mesophase transition temperatures but also the layer-spacing length (d_1) and the side-chain distance (d_2). The long- and short-range orders can remain to some extent above the isotropization temperature and below the melting point. The polymer PS3BDBE3 decomposed in air 20°C above the isotropization temperature and lost its short range orders as detected by the X-ray diffraction analysis.

1. Introduction

Side chain liquid crystalline (SCLC) polymers have been extensively studied during the last few years [1-4]. Thermotropic SCLC polymers, owing to their particular properties, have been paid attention to as potential advanced materials for specialty applications [5-15]. Synthesis, structure-property relations, and applications were concisely reviewed by Varshney [16] and Gray *et al.* [17]. Owing to their high viscosity, broad molecular weight distribution, and polycrystalline and amorphous material coexistence, the LC nature of the thermotropic polymer was usually established through a combination of the following methods [18]: (a) differential scanning calorimetry (DSC), (b) optical pattern or texture observations, (c) miscibility studies, (d) X-ray investigations, and (e) the possibility of inducing significant molecular orientations by magnetic or electric fields. Among them, the X-ray diffraction method is powerful for the qualitative determination for the crystalline and LC microstructure. Gemmell *et al.* [19, 20] studied the side chain acrylate and methacrylate LC polymers containing the 4'-alkylbiphenyl-4-yl and 4'-cyanobiphenyl-4-yl substituents as a side group by X-ray techniques. They reported that increasing the anisotropy in the biphenyl side chain by suitable terminal substituents greatly increased the propensity for smectic-type ordering of the side chain. Meanwhile, the smectic-like side chain ordering is affected by the methyl substituent on the main chain and the polarity of the terminal group. Sagane and Lens [21] reported that poly(vinyl ethers) with alkoxy biphenyl and cyanobiphenyl side chains show mesophases and they demonstrated that the types of mesophase texture and mesophase microstructure are related to the polarity and lengths of the terminal substituents.

Selectivity, column efficiency, and thermal stability are the important factors that are used in the high resolution gas chromatography packed stationary phase materials [12]. Thus, it seemed to us that a study of liquid crystalline microstructure and thermal stability would be useful, especially in view of this application. In the previous study [22], 4'-oligo (ethylene oxide) monomethyl ether carbonyl biphenyl-4-yl 4-(alkenyloxy) benzoate SCLC polysiloxane polymers were prepared. Those polymers only show the grain-like texture in the optical microscopy but do not develop characteristic smectic textures.

*Author for correspondence.

0267-8292/96 $12·00

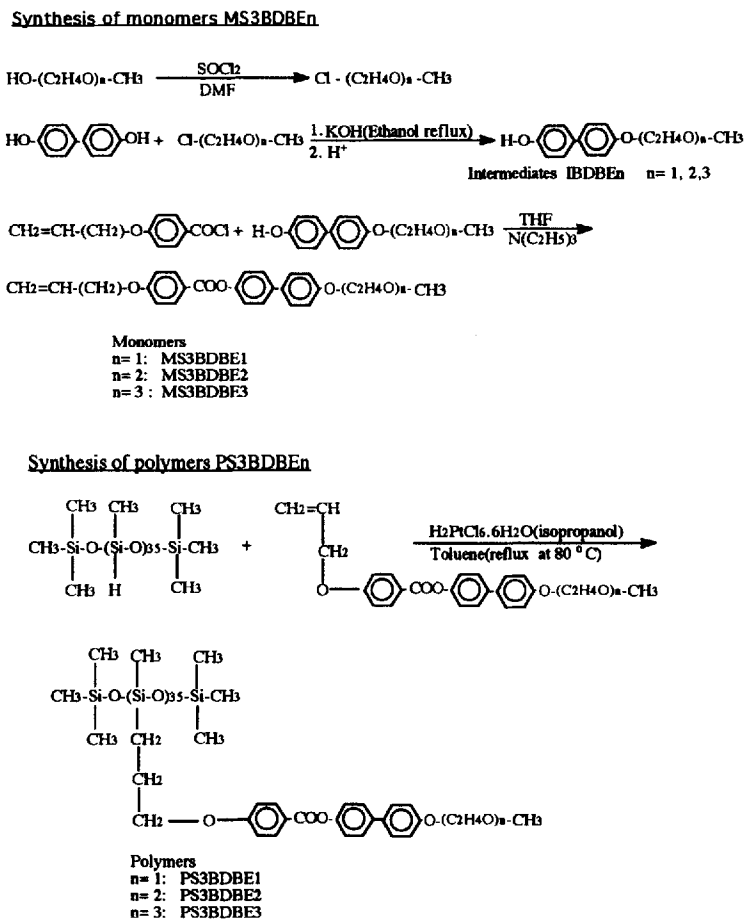

Scheme 1. Procedure for the preparation of the monomers MS3BDBE*n* and the polysiloxane polymers PS3BDBE*n*.

In this study, we will present the results of the mesophase texture, microstructure, and thermal stability by using X-ray diffraction, polarized optical microscopy, and DSC thermal analysis.

2. Results and discussion

Scheme 1 shows the preparations of the monomers and polymers in detail. The identification of the monomers and polymers by the ^{1}H NMR and ^{13}C NMR was described elsewhere [22].

Figures 1 and 2 (*a*) and (*b*), respectively, show the DSC thermograms for the monomers MS3BDBE*n* and polymers PS3BDBE*n* in this study. Figure 3 shows the mesophase texture for the monomer MS3BDBE3. Figures 4 and 5 (*a*), (*b*), (*c*), and (*d*), respectively, show the mesophase textures for the polymer PS3BDBE1 and PS3BDBE3 cooling from the isotropization temperature. Tables 1 and 2 summarize the mesophase types, transition temperatures, and thermodynamic parameters for the monomers and the polymers, respectively. As can be seen, all the monomers show the nematic phase only and the terminal length of the ethylene glycol monomethyl ether group has influenced the transition temperatures and the change of enthalpy and entropy of the monomers. The longer the oligo (ethylene oxide) unit, the lower are the nematic phase transition temperature, the smaller are changes of enthalpy and entropy, and the narrower the nematic temperature range. All the polymers exhibit fine-grain smectic textures and/or schlieren-like nematic textures in the polarized optical microscopy, regardless of having their precursor monomers showing nematic phase only. The polymer PS3BDBE3 with 3 oligo (ethylene oxide) units shows a glass transition at 78°C in the DSC thermograms, whereas PS3BDBE1 and PS3BDBE2 containing 1 and 2 oligo (ethylene oxide) units, respectively, show crystalline melting points only. The polymer PS3BDBE3 shows two mesophase transition temperatures at 160·4°C and 191·7°C in the heating thermograms and two mesophase transition temperatures at 179·2°C and 154·5°C in the cooling thermograms. We did not find any significant difference of the fine-grain mesophase texture in the

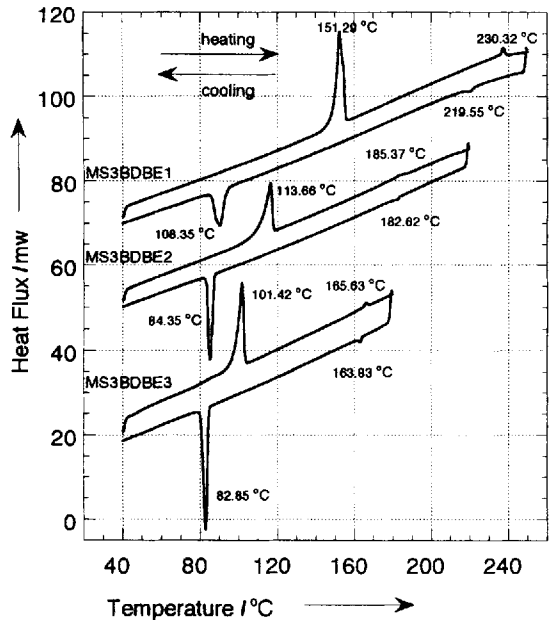

Figure 1. DSC thermograms of the monomers MS3BDBEn in the heating and cooling experiment (scanning rate of 10°C min^{-1}).

polarized optical microscopy (see figure 4 (a)-(d)) at the above two mesophase transition temperatures. From these results given in table 2, it can be seen that the isotropization transition temperatures are sensitive to the number of oligo (ethylene oxide) units in the terminal group. The polymer PS3BDBE2 containing 2 oligo (ethylene oxide) units shows the lowest isotropization transition temperature. These results with a zigzag behaviour are not similar to those results [26] containing a carboxyl biphenyl benzoate ester mesogenic core with a carboxyl oligo (ethylene oxide) monomethyl ether group. To our knowledge this is the first observation of an 'odd-even' effect on the isotropization transition temperature for the oligo (ethylene oxide) unit in the terminal group.

Figure 6 shows the X-ray diffraction diagrams of the polymer PS3BDBE1 at various temperatures after cooling from 280°C in a vacuum. It shows only a wide angle broad reflection at 18·09°. When the temperature is further cooled down to 240°C. A weak and narrow small angle reflection at $2\theta = 3{\cdot}33°$ and a broad wide angle reflection at $2\theta = 18{\cdot}09°$ are found. The reflection at the small angle became relatively symmetric, narrow and strong and shifted to 3·45° when the temperature was further cooled to 160°C, whereas the intensity of the broad reflection did not significantly change but shifted to a higher angle. The reflection at the small angle of a 2θ is characteristic of a smectic phase. It is related to the layer spacing d_1 [23]. Meanwhile, the broad reflection peak at $2\theta = 18$–$20°$ provides the side chain distance d_2 [24] of the LC polymer. From the DSC thermograms (see figure 2 (b)), one knows that there is an isotropic transition temperature (T_{IN}) at 262·8°C, a mesophase transition temperature T_{NS} at 204·8°C, and two melting transition temperatures (T_{SCr}) at 128·8°C

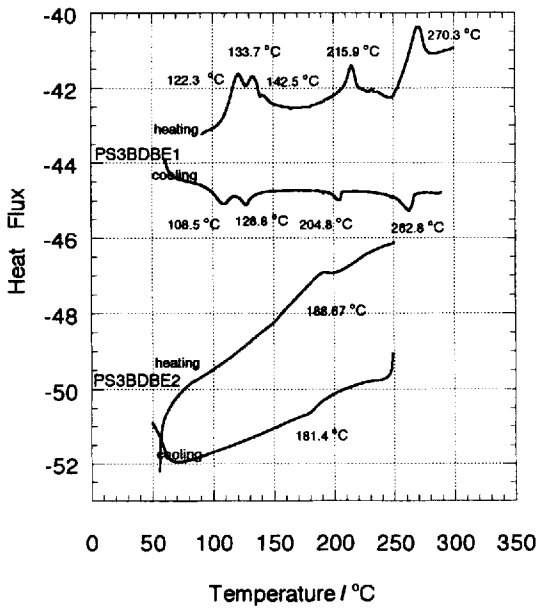

(a)

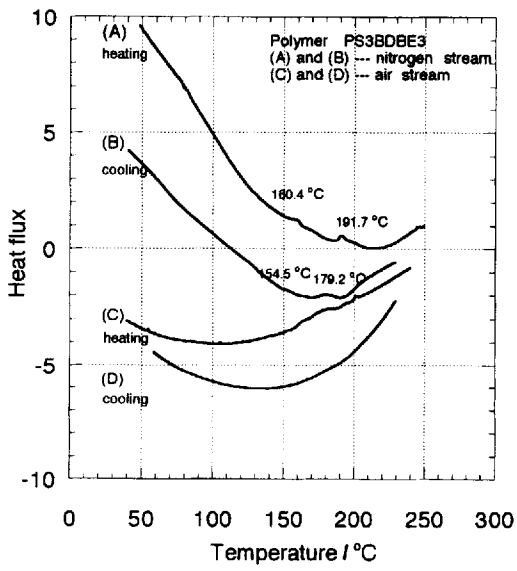

(b)

Figure 2. (a) DSC thermograms of the polymers PS3BDBE1 and, PS3BDBE2 (scanning rate of 10°C min^{-1}), and (b) DSC thermograms of the polymer PS3BDBE3 in the nitrogen and air stream (scanning rate 10°C min^{1}).

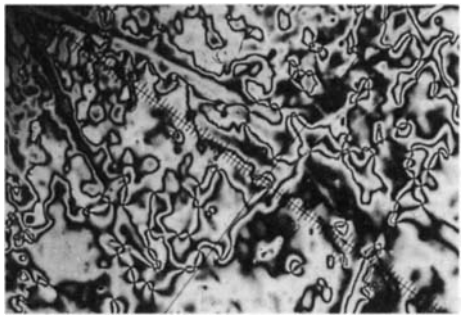

Figure 3. Polarized optical micrograph presenting the nematic schlieren texture of monomer MS3BDBE3 at 210°C (cooling scan, ×200).

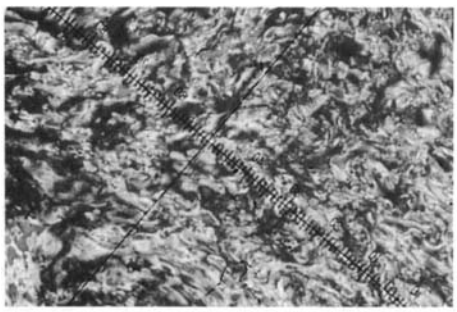

(*a*)

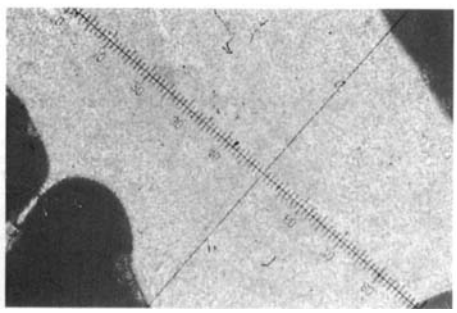

(*b*)

Figure 4. Polarized optical micrographs presenting the (*a*) nematic texture (275°C) and, (*b*) smectic texture (240°C) for the polymer PS3BDBE1 (cooling scan, ×200).

and 108·5°C. From the X-ray diffraction patterns and DSC thermograms, it is revealed that the short-range order (smectic phase structure) of the side chain has begun to develop in the nematic phase temperature region. As the temperature is further cooled down to the temperature 120°C (below T_{SCr}), the intensity and position of the small angle reflection do not change, whereas the intensity of the broad reflection becomes relatively symmetric, narrow, and strong. If the temperature is further cooled down to 40°C, the intensity and position of the small angle and the intensity of the wide angle reflection do not change, whereas the reflection peak position shifts to the higher angle. It indicated that d_2 is continuing to become smaller in the above temperature range (for example, the lower the temperature, the closer the side chain groups). This may have resulted from the effect of the secondary interaction forces imposing on the side chain, because the secondary intermolecular interaction forces increase with decreasing temperature. It is noted that as the temperature was continuously cooled down to below T_{Cr}, the smectic characteristic of the X-ray diffraction pattern remained. This fact reflects that the smectic phase structure was 'frozen' below T_{Cr}. When the temperature was heated to 280°C, 260°C, and 150°C from the crystalline state (as shown in figure 6(*b*)) the intensity, position, and shape of X-ray reflection patterns are the same as results from experiments cooling through 280°C, 260°C, and 150°C. It is revealed that the LC phase of the polymer PS3BDBE1 is reversible. Using the Bragg equation, both d_1 and d_2 were obtained (see table 3). The d_2 values obtained were around 4·5–4·7 Å. It is interesting to find that the d_2 values obtained are close to those of side chain LC polyacrylates and polymethacrylates reported by Gemmell *et al.* [19, 20] and Frosini *et al.* [25]. It is noteworthy that the bond angle ($\theta = 142°$) and the bond length ($L = 1{\cdot}62$ Å) of -Si-O-Si- are larger than those of -C-C-C- in acrylates and methacrylates, which are about 109·5° and $L = 1{\cdot}53$ Å. The layer spacings decreased in the range of 25–43 Å. The increase of terminal length tended to increase d_1. It was observed that the d_1 values are not larger than those of acrylic LC polymers, in spite of the lengths of the side chains being much longer than those of the side chains of acrylic LC polymers reported by Gemmell *et al.* [19, 20]. The total length of side chains is estimated (see table 3), assuming that they are in the fully extended conformations (see scheme 2(*a*)). It is noteworthy that those layer spacing distances are much smaller than twice the side chain length of the fully extended conformations. Therefore, the two-layer end-on packing or the two-layer packing with overlapping tails model [23] seemed unable to ascribe the structure of the side chain LC polysiloxanes concerned. Furthermore, the tilted packing model (in scheme 2(*b*) or 2(*c*)) proposed for the polymers is obtained in this study.

Figure 7 shows the X-ray diffraction patterns of the polymer PS3BDBE3 at various temperature cooling from 220°C (above the isotropization temperature 20°C) in a vacuum. It shows a broad reflection at the wide angle region 18·3°C and a sharp and narrow reflection at $2\theta = 2{\cdot}08°$ at 200°C. When the temperature was further cooled to 180°C, the intensity of the small angle became weak and there appears a second small angle reflection at

$2\theta = 3{\cdot}54°$. It is indicated that the intensity of the small angle at $2\theta = 2{\cdot}08°$ becomes smaller and shifts to the higher angle, whereas the intensity of the reflection peak at $2\theta = 3{\cdot}54°$ becomes larger and shifts to the smaller angle in the temperature range 180–30°C. From the cooling thermograms (see figure 2 (*b*) curve (B) for the polymer PS3BDBE3), one knows that there are two mesophase transition temperatures at 190·4°C and 163°C. However, one cannot observe a texture change in polarized optical microscopy. Figure 8 illustrates the ^{1}H NMR spectrum for the polymer PS3BDBE3. The resonance peaks of the alkene (C–C<u>H</u>–, 6·05 ppm) and (C<u>H</u>$_2$-C–, 5·50 ppm) and the poly(methylhydrosiloxane) backbone (Si–<u>H</u>, 4·8 ppm) group cannot be found. Obviously, there is no residual monomer in the polymer material. Therefore, the two mesophase transition temperatures seem to ascribe to two kinds of layer spacing of the smectic structure. When the temperature was reheated to 200°C (from the reflection patterns (see figure 7)), one finds that the intensity and position of the small angle has recovered. The above phenomena, therefore, illustrate that the smectic phase structure of the polymer PS3BDBE3 is reversible.

Finally, we took the polymer PS3BDBE3 to study the effect of heat treatment on the thermal stability of the polymer. Before doing the X-ray diffraction measurement, the polymer PS3BDBE3 was coated onto the platinum hot plate at 210°C and ambient pressure, and the X-ray diffraction investigations were then performed on the preheated sample. Comparing the reflection patterns in figure 7 with the 210°C curve of figure 9, one can find that both have a broad reflection in the wide angle region 18·3° and a sharp and narrow reflection at $2\theta = 2{\cdot}08°$. Obviously, the pressure condition (vacuum or ambient) did not affect the layer spacing or the side chain distance of the liquid crystalline structure. After the sample was heated at 220°C and ambient pressure for three minutes. In examining the X-ray diffraction patterns (220°C–25°C), one can find that the small angle reflection peak almost disappears whereas the wide angle reflection does not significantly change. From the DSC cooling thermograms (see figure 2 (*b*), curve (D)), one finds that the two mesophase transition temperatures at 190·4°C and at 163·2°C almost disappear. From the above results, it is found that the polymer PS3BDBE3 decomposes in ambient pressure at 220°C and loses its LC short range order.

3. Experimental

3.1. *Materials*

p-Hydroxybenzoic acid, 2-methoxyethanol, diethylene glycol monomethyl ether, triethylene glycol monomethyl ether, allyl bromide and 4,4-dihydroxybiphenyl (from Tokyo Chemical Industry Co., Ltd) were used as received. Polymethylhydrosiloxanes (with $\overline{DP} \approx 35$, $\overline{M}_w \approx 2268$) and hexachloroplatinic acid ($H_2Pt_2Cl_6 \cdot 6H_2O$)

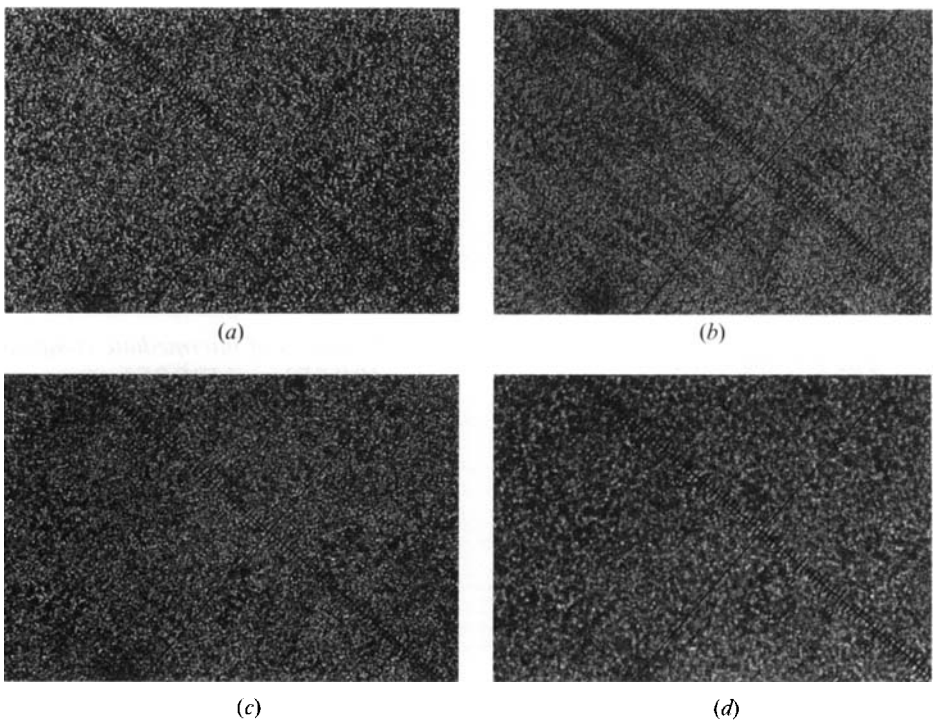

Figure 5. Polarized optical micrographs presenting the (*a*) smectic texture (190°C), (*b*) smectic texture (170°C), (*c*) smectic texture (150°C), and (*d*) smectic texture (100°C) for the polymer PS3BDBE3 (cooling scan, × 200).

Table 1. Thermal transition temperatures (°C)[a], mesophase types[b], and the changes in enthalpy (ΔH) and entropy (ΔS) (in parentheses) associated with the transitions (in $J g^{-1}$ and $mJ g^{-1} K^{-1}$, respectively).

Monomer	Cooling Heating
MS3BDBE1	Cr 151·29 N 230·32(4·92/9·77) I I 219·55 (2·95/5·99) N 108·35 Cr
MS3BDBE2	Cr 113·66 N 185·37 (1·51/3·29) I I 182·62 (1·23/2·70) N 84·35 Cr
MS3BDBE3	Cr 101·42 N 165·63 (1·08/2·46) I I 163·83 (0·93/2·13) N 82·85 Cr

[a] Heating and cooling rate were 10°C min^{-1}.
[b] Mesophase types were determined by polarized optical microscopy and X-ray diffraction.
Cr: crystalline; S: smectic phase; N: nematic phase; I: isotropic phase.

Table 2. Thermal transition temperatures (°C)[a], mesophase types[b], and the changes in enthalpy (ΔH) and entropy (ΔS) (in parentheses) associated with the transitions (in $J g^{-1}$ and $mJ g^{-1} K^{-1}$, respectively).

Polymer	Cooling Heating
PE1S3	g 29 S 251 (2·29/4·4) I I 248 (1·8/3·45) S 24 g
PE2S3	g 22 S 187 (2·21/4·8) I I 184 (2·3/5·03) S 18 g
PS3BDBE0	Cr 132 N 281·2 I I 275·8 (1·76/3·21) N 112 Cr
PS3BDBE1	Cr 111 S 263·5 I I 255·4 S 107 Cr
PS3BDBE2	Cr 77·9 S 188·6 I I 181·4 S 75·6 g
PS3 BDBE3	g 82·9 S_1 160·4 S_2 191·7 I I 179·2 S_2 154·5 S_1 75 G
PS3BE1DB	Cr 81·08 I 72·23 Cr
PS3BE2DB	Cr 97·33 I I 81·54 Cr
PS3BE3DB	Cr 65·91 I I 42·2 Cr
PS8BE2DB	Cr 85·56 I I 73·15 Cr

[a] Heating and cooling rate were 10°C min^{1}.
[b] Mesophase types were determined by polarized optical microscopy and X-ray diffraction.
Cr: crystalline; S: smectic phase; N: nematic phase; I: isotropic phase; G: glass.

(from E. Merck Ltd) were used as received. Toluene, used as solvent in the hydrosilylation reaction, was refluxed over sodium and then distilled under nitrogen.

3.2. *Monomer synthesis [MS3BDBEn (n = 1,2,3)]*

Synthesis of monomers MS3BDBE*n* and polymers PS3BDBE*n* are outlined in scheme 1.

3.2.1. *Synthesis of 2-chloroethylene methyl ether, 2-(2-chloroethoxy) ethylene methyl ether, and 2-(2-(2-chloroethoxy)ethoxy) ethylene methyl ether*

2-Chloroethylene methyl ether, 2-(2-chloroethoxy) ethylene methyl ether, and 2-(2-(2-chloroethoxy)ethoxy) ethylene methyl ether were respectively synthesized from 2-methoxyethanol, diethylene glycol monomethyl ether, and triethylene glycol monomethyl ether by using the chloride substitution reaction. The synthesis of 2-chloroethylene methyl ether is illustrated as follows: 2-methoxyethanol 20 g (0·263 mol) was placed in a 250 ml two neck round-bottomed flask, equipped with an addition funnel and a HCl absorption apparatus. Thionyl chloride 60 ml was added slowly, followed by 5 drops of DMF. The reaction mixture was then refluxed at 70°C for 5 h. After the reaction was complete the dark brown solution was poured into 200 ml distilled water. This solution was extracted twice with 100 ml CH_2Cl_2. The organic layer was washed (2 ×) with saturated sodium bicarbonate solution, with water (2 ×), and then dried over anhydrous magnesium sulphate ($MgSO_4$). The CH_2Cl_2 was removed with a rotary evaporator under reduced pressure. The residual solution was further purified by reduced pressure distillation. 21 g 2-chloroethylene methyl ether was finally obtained (yield 84·5 per cent). The characteristic IR absorption peak of the hydroxyl group at 3450 cm^{-1} was not observed, indicating the hydroxyl group was completely substituted by chloride. 2-(2-Chloroethoxy) ethylene methyl ether (80 per cent) and 2-(2-(2-chloroethoxy)ethoxy) ethylene methyl ether (81 per cent) were obtained consistently.

3.2.2. *Synthesis of intermediate compounds IBDBE1, IBDBE2, and IBDBE3*

The intermediate compounds IBDBE1, IBDBE2, and IBDBE3 were synthesized by the same method. As an example, the synthesis of IBDBE2 is illustrated as follows: 4,4'-dihydroxybiphenyl 10 g (0.054 mol) and NaOH 4·32 g (1·08 mol) were placed in a 500 ml round-bottomed flask which contained 120 ml ethanol. The reaction solution was refluxed until the 4,4'-dihydroxybiphenyl became the sodium salt (*c.* 0·5 h). 2-(2-Chloroethoxy) ethylene methyl ester (8·23 g, 0·059 mol) was added to the brown solution and was refluxed overnight (the mixture solution became light yellow). The solution was poured into water and acidified with HCl

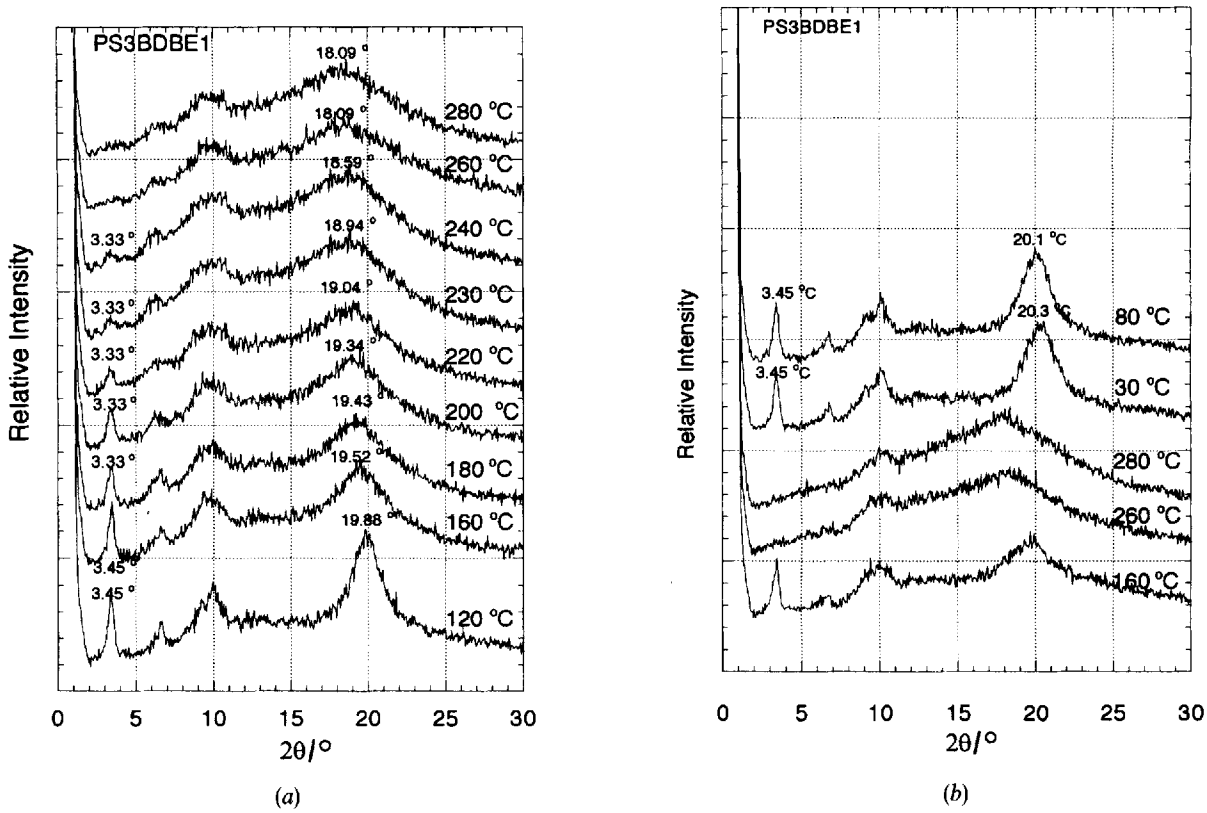

Figure 6. Variation of the intensity of the diffraction with the temperature for (*a*) the polymer PS3BDBE1, and (*b*) the polymer PS3BDBE1.

Table 3. X-ray diffraction for the polymers in this study.

	Small angle		Wide angle		Calculated length of anisotropic unit/Å
Polymer	2θ/°	d_1/Å	2θ/°	d_2/Å	
PS3BDBE1	3·43	25·8	19·7	4·5	25·0
PS3BDBE2	2·36	37·4	19·1	4·6	27·4
PS3BDBE3	2·08	42·5	18·9	4·7	30·6

acid. The precipitated product was filtered, washed with water, and dried in a vacuum oven. The crude product was further purified in a silica gel packed column, with CH_2Cl_2/*n*-hexane/methanol (35v/15v/2v) as the mobile phase to obtain 7·0 g of pure product (yield 45 per cent; m.p. 153°C). IBDBE1: CH_2Cl_2/*n*-hexane/methanol (35v/15v/1v) was the mobile phase (yield 52 per cent; m.p. 113°C). IBDBE3: CH_2Cl_2/*n*-hexane/methanol (35v/15v/3v) was the mobile phase (yield 49 per cent; m.p. 109°C).

3.2.3. *Synthesis of monomers MS3BDBE1, MS3BDBE2, and MS3BDBE3*

All the monomers were synthesized by the same procedure. As an example, the synthesis of MS3BDBE2 is illustrated as follows: 0·0267 mol 4-allyloxy benzoic acid (3) (4·753 g) and 16 ml thionyl chloride containing a drop of dimethylformamide (DMF) were reacted at 50°C until the solution became clear (*c.* 3 h). The excess thionyl chloride was removed by a rotary evaporator equipped with a reduced pressure water pump to obtain yellow, viscous 4-allyloxybenzoyl chloride. The acid chloride was dissolved in 5 ml THF, and slowly added to a solution of 0·0243 mol (7·0 g) IBDBE2 compound with an excess molar ratio of dry triethylamine and 50 ml of THF in an ice bath. The THF and triethylamine were removed by a rotary evaporator under reduced pressure. The residual material was purified on a silica gel packed column with CH_2Cl_2/*n*-hexane/methanol (40v/10v/2v) as the mobile phase to obtain a pure produce 6·35 g (yield 60 per cent); MS3BDBE1: CH_2Cl_2/*n*-hexane/methanol (40v/10v/1v) was the mobile phase (yield 65 per cent). MS3BDBE3: CH_2Cl_2/*n*-hexane/methanol (40v/10v/3v) was the mobile phase (yield 62 per cent).

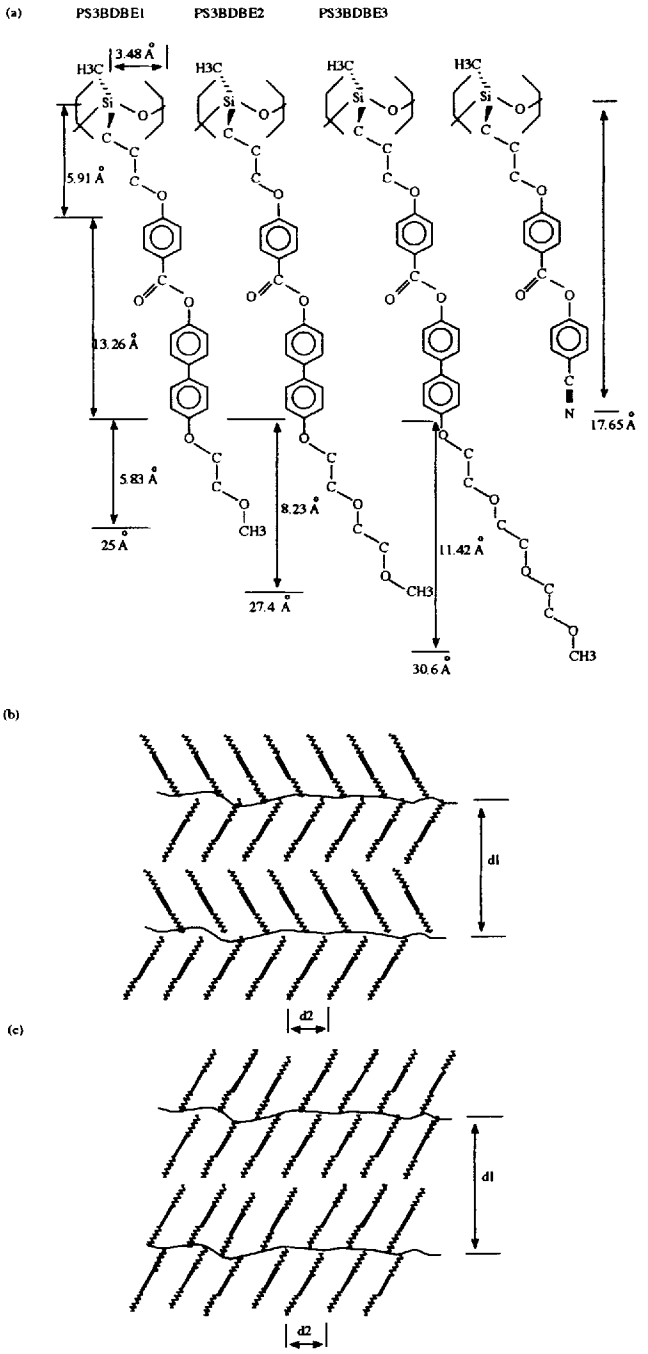

Scheme 2. (*a*) the molecular structure of the polymers PS3BDBE*n* in this study, (*b*) the representation of the structural arrangement of the smectic C, and (*c*) the representation of the structural arrangement of the smectic C phase.

The characteristic ^{1}H NMR and ^{13}C NMR chemical shifts of the monomers MS3BDBE*n* are described elsewhere [22]. The transition temperatures, mesophase types, and thermodynamics parameters of the monomers are summarized in table 1.

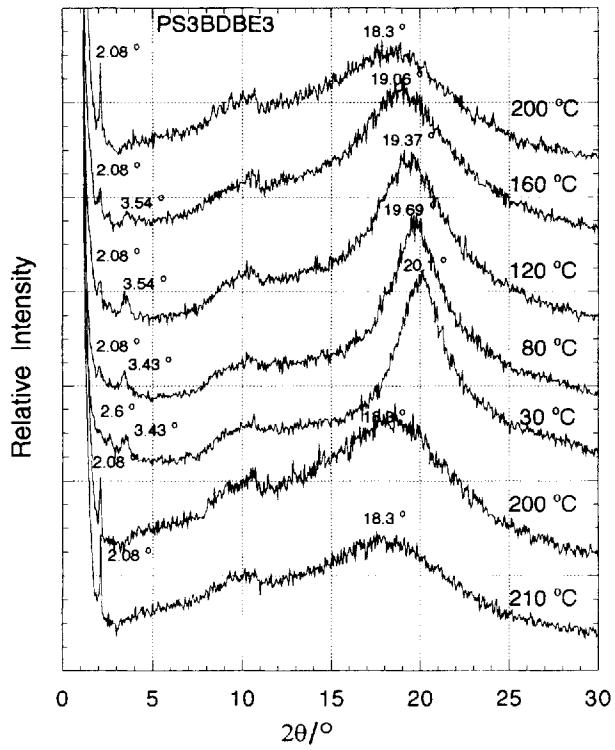

Figure 7. Variation of the intensity of the diffraction with the temperature for the polymer PS3BDBE3 under vacuum.

3.3. *Polymer synthesis*

1 g MS3BDBE3 and 0·136 g polymethylhydrosiloxane were dissolved in 10 ml of sodium-dried toluene. One drop of 5×10^{-3} M $H_2PtCl_6 \cdot 6H_2O$ solution (in isopropanol) as the grafting catalyst was added to the above solution. The reaction temperature was kept at 80°C under a nitrogen stream. The reaction was continued until the IR absorption peak of Si–H disappeared. The product was subsequently purified through methanol precipitation and CH_2Cl_2 redissolution several times. It was then dried in a vacuum oven at room temperature. The transition temperatures, liquid crystalline phase, and thermodynamics parameters of the polymers are summarized in table 2.

3.4. *Characterization of thermal properties and liquid crystalline textures for monomers and polymers*

The transition temperatures of the monomers and the polymers were studied using a Perkin–Elmer DSC-7 differential scanning calorimeter with a central processor and an intracooler II for the cooling experiment. Dry nitrogen and air purge gases were used, respectively, for the thermal degradation experiments. The flow rate of the purge gases was 40 cm^3 min^{-1}. The liquid crystalline textures of the monomers and polymers were observed

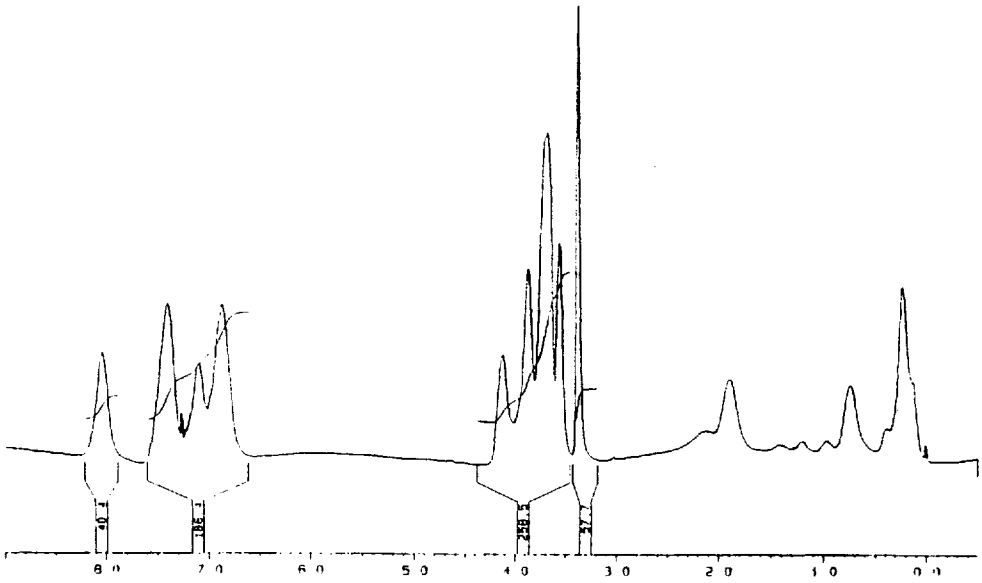

Figure 8. 200 MHz ^{1}H NMR spectrum for the polymer PS3BDBE3.

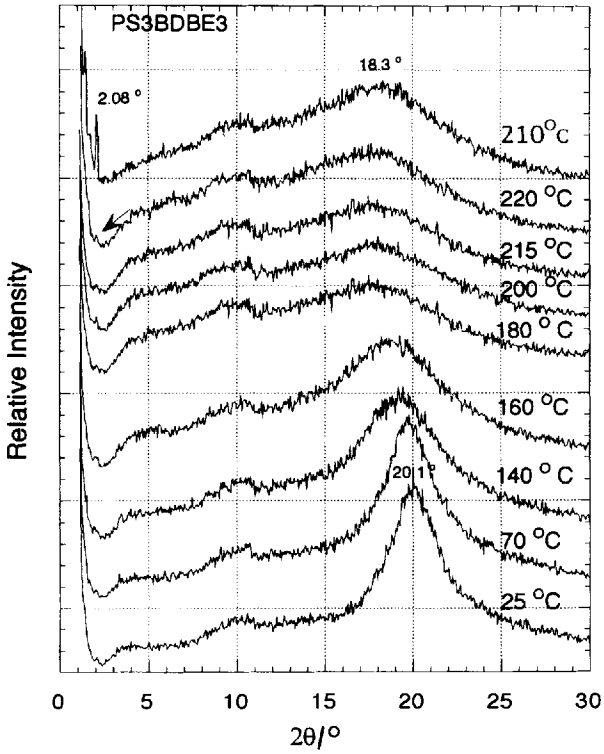

Figure 9. Variation of the intensity of the diffraction with the temperature for the polymer PS3BDBE3 at ambient pressure.

with an Olympus BH-2 polarized optical microscope with a Linkam THMS 600 hot stage and a TP 92 central control processor.

3.5. *Microstructure and thermal degradation experiments*

Microstructure and thermal degradation experiments were performed with a Siemens Diffraktometer D5000 X-ray apparatus (40 kV, 30 mA). Nickel-filtered CuK$_\alpha$ radiation was used as the incident X-ray beam. The intensity of the scattered X-rays was measured by a scintillation counter. The diffractometer scanned over a range of $1° < 2\theta < 30°$ with a scanning speed of 0·05°/0·1 s. The polymer sample was coated on a 15 cm (length) × 2 cm (width) controllable platinum hot plate. The thickness of the sample was about 1 mm. The platinum hot plate was put in a vacuum chamber (1×10^{-5} torr) or at ambient pressure for comparing the thermal degradation results.

We are grateful to the National Science Council of The Republic of China for financial support for this work (NSC-83-0117-C-230-001E). We also thank Dr Bing-Hwai Hwang and Miss Show-Yueh Lee for their help in carrying out the X-ray diffraction measurements.

References

[1] Ging-Ho Hsiue, and Jr-Hong Chen, 1995, *Macromolecules*, **28**, 4366.
[2] Lu, Y. H., and Hsu, C. S., 1995, *Macromolecules*, **28**, 1673.
[3] Ringsdorf, H., and Schneller, A., 1982, *Makromol. Chem., rap. Commun.*, **3**, 557.
[4] Rodriguez-Parada, J. M., and Percec, V., 1987, *J. Polym. Sci., Polym. Chem.*, **25**, 2269.
[5] Coles, H. J., and Simon, R., 1985, *Polymer*, **26**, 1801.

[6] SHIBAEV, V. P., IVANOV, S. A., KOSTROMIN, S. G., PLATE, N. A., VETROV, V. Y., and YAKOVLEV, I. A., 1983, *Polymer Commun.*, **24,** 364.
[7] MCARDLE, C. B., CLARK, M. G., GRAY, G. W., HAWS, C. M., LACEY, D., NESTOR, G., PARKER, A., TOYNE, K. J., and WILTSHIRE, M. C. K., 1987, *Liq. Cryst.*, **2,** 573.
[8] FINKELMANN, H., and REHAGE, G., 1982, *Makromol. Chem., rap. Commun.*, **3,** 859.
[9] EBERLE, H.-J., MILLER, A., and KREUZER, F.-H., 1989, *Liq. Cryst.*, **5,** 907.
[10] BONE, M. F., GRAY, G. W., LACEY, D., GEMMELL, P. A., TOYNE, K. J., CHAN, L. K. M., COATES, D., CONSTANT, J., and BRADSHAW, M. J., 1988, *Mol. Cryst. liq. Cryst.*, **164,** 117.
[11] JANINI, G. M., MUSCHIK, G. M., ISSAQ, H. J., and LAUB, R. J., 1988, *Anal. Chem.*, **60,** 1119.
[12] MARKIDES, KARIN E., NISHIOKA, MASAHARU, TARBET, BRIAN J., BRADSHAW, JERALD S., and LEE, M. L., 1985, *Anal. Chem.*, **57,** 1296.
[13] JONES, B. A., BRADSHAW, J. S., NISHIOKA, M., and LEE, M. L., 1984, *J. org. Chem.*, **49,** 4947.
[14] KONG, ROBERT C., LEE, MILTON L., TOMINAGA, YOSHINORI, PRATAP, RAM, IWAO, MASATOMO, and CASTLE, RAYMOND N., 1982, *Anal. Chem.*, **54,** 1802.
[15] HAKY, J. E., and MUSCHIK, G. M., 1981, *J. Chromatogr.*, **214,** 161.
[16] VARSHNEY, S. K., 1986, *Macromol. chem. Phys.*, **C26,** 551.
[17] GRAY, G. W., HAWTHORNE, W. D., HILL, J. S., WHITE, M. S., NESTOR, G., LACEY, D., and LEE, M. S. K., 1989, *Polymer*, **30,** 964.
[18] GRIFFIN, A. C., *et al.*, 1985, *Polymeric Liquid Crystals*, edited by A. Blumstein (New York, London: Plenum Press), p. 21.
[19] GEMMELL, P. A., GRAY, G. W., ALIMOGLU, A. K., LACEY, D., and LEDWITH, A., 1985, *Polymer*, **26,** 615.
[20] ÄLIMOGLU, A. K., LEDWITH, A., GEMMELL, P. A., GRAY, G. W., and LACEY, D., 1984, *Polymer*, **25,** 1342.
[21] SAGANE, T., and LENZ, R. W., 1989, *Polymer*, **30,** 2269.
[22] GUO-PING CHANG-CHIEN, and JEN-FENG KUO, 1995, *J. Appl. Sci.* in the press.
[23] WUNDERLICH, B., GREBOWICZ, J., DOBB, M. G., MCINTYRE, J. E., FINKELMANN, H., REHAGE, G., SHIBAEV, V. P., and PLATÉ, N. A., 1984, *Advances in Polymer Science*, 60/61, edited by M. Gordon (Berlin, Heidelberg, New York, Tokyo: Springer-Verlag), p. 193.
[24] GRAY, G. W., HARTLEY, J. B., and JONES, B., 1955, *J. chem. Soc.*, **2,** 1412.
[25] FROSINI, V., LEVITA, G., LUPINACCI, D., and MAGAGNINI, P. L., 1981, *Mol. Cryst. liq. Cryst.*, **66,** 21.
[26] GUO-PING CHANG-CHIEN, JEN-FENG KUO, and CHUH-YUNG CHEN, 1993, *J. Polym. Sci. Polym. Chem.*, **31,** 2423.